Available online at www.sciencedirect.com
SCIENCE DIRECT®
Journal of Solid State Chemistry 177 (2004) 1567–1574
JOURNAL OF SOLID STATE CHEMISTRY
http://elsevier.com/locate/jssc

Synthesis, crystal structure and electrical characterization of $Cs_4[(UO_2)_2(V_2O_7)O_2]$, a uranyl divanadate with chains of corner-sharing uranyl square bipyramids

S. Obbade,* C. Dion, M. Saadi, and F. Abraham

Laboratoire de Cristallochimie et Physicochimie du Solide, UMR CNRS 8012, ENSCL-USTL, B.P. 108, F-59652 Villeneuve d'Ascq Cedex, France

Received 23 September 2003; received in revised form 1 December 2003; accepted 9 December 2003

Abstract

A new cesium uranyl vanadate $Cs_4[(UO_2)_2(V_2O_7)O_2]$ has been synthesized by solid-state reaction and its structure determined from single-crystal X-ray diffraction data. It crystallizes in the orthorhombic symmetry with space group *Pmmn* and following cell parameters: $a = 8.4828(15)$ Å, $b = 13.426(2)$ Å and $c = 7.1366(13)$ Å, $V = 812.8(3)$ Å^3, $Z = 2$ with $\rho_{mes} = 5.39(2)$ g/cm^3 and $\rho_{cal} = 5.38(1)$ g/cm^3. A full-matrix least-squares refinement on the basis of F^2 yielded $R_1 = 0.027$ and w$R_2 = 0.066$ for 62 parameters with 636 independent reflections with $I \geqslant 2\sigma(I)$ collected on a BRUKER AXS diffractometer with Mo$K\alpha$ radiation and a charge-coupled device detector. The crystal structure is characterized by $^2_\infty[(UO_2)_2(V_2O_7)O_2]^{4-}$ corrugated layers parallel to (001). The layers are built up from distorted $(UO_2)O_4$ octahedra and divanadate V_2O_7 units resulting from two VO_4 tetrahedra sharing corner. The distorted uranyl octahedra $(UO_2)O_4$ are linked by corners to form infinite $^1_\infty[UO_5]^{4-}$ chains parallel to the *a*-axis. These chains are linked together by symmetrical divanadate units sharing two corners with each chain, the two last corners being oriented towards the same interlayer. The cohesion of the structure is assured by interlayer Cs^+ ions. Their mobility within the interlayer space gives rise to a cationic conductivity with an important jump between 635°C and 680°C. $Cs_4[(UO_2)_2(V_2O_7)O_2]$ is readily decomposed by water at 60°C to form the Cs-carnotite analog $Cs_2(UO_2)_2(V_2O_8)$ compound.

Keywords: Uranyl divanadate; Crystal structure refinement; Layered compound; Solid-state synthesis; Cationic conductivity

1. Introduction

Several previous studies of hexavalent uranium-containing compounds showed that they exhibit a strong tendency to adopt layered structures due to the presence of dioxo $(UO_2)^{2+}$ units that generally prevents the third dimension of linkage [1–5]. To illustrate this phenomenon, a comparison and hierarchy of crystal structures of minerals and inorganic uranyl phases from a topological viewpoint, indicate that a large number of these compounds crystallize in structures with infinite sheets of connected polyhedra [1]. In other cases, infinite ribbons, infinite chains, finite clusters or frameworks of polyhedra are observed. In these materials, the hexavalent uranium U(VI) cation is usually present as an approximately linear $(UO_2)^{2+}$ uranyl ion, coordinated in the equatorial plane by four, five or six ligands ($\phi = O^{2-}$, OH^-, Cl^-, H_2O, etc.) to give tetragonal bipyramids $(UO_2)\phi_4$, pentagonal bipyramids $(UO_2)\phi_5$ or hexagonal bipyramids $(UO_2)\phi_6$, respectively. Among these compounds, the association of uranyl polyhedra, sharing corners and/or edges of equatorial polygons, directly or through associated various oxoanions (BO_3^{3-}, CO_3^{2-}, NO_3^-, SiO_4^{4-}, GeO_4^{4-}, PO_4^{3-}, AsO_4^{3-}, SO_4^{2-}, $P_2O_7^{4-}$, SeO_3^{2-}, VO_4^{3-}, NbO_4^{3-}, CrO_4^{2-}, MoO_4^{2-}, $V_2O_8^{6-}$, $W_2O_8^{4-}$, etc.), gives varied and interesting crystal structures [1,2].

Layered structures are generally favorable for a good ionic electrical conductivity assured by the mobility of interlayer cations. This property has been initially observed in β alumina where Na^+ ions are able to move freely within the conduction planes between the dense spinel blocks [6]. It was also observed in $H(UO_2)(PO_4)$, $4H_2O$, HUP, which is among the best electrical protonic conductors known currently, and has

*Corresponding author. Fax: 33-3-20-43-68-14.
E-mail address: obbade@ensc-lille.fr (S. Obbade).

0022-4596/$ - see front matter © 2003 Elsevier Inc. All rights reserved.
doi:10.1016/j.jssc.2003.12.007

received much attention for its potential applications in electrochemical domain [7–12]. Its high electrical conductivity is related with protons H^+ which can jump between interlayer water molecules.

From this viewpoint, several layered uranyl vanadates families are known. We have already studied monovalent metal uranyl vanadates with a molar ratio U/V = 1 [3–5]. These materials belong to the large class of layered compounds of general formula $M^{n+}_{1/n}UO_2XO_4 \cdot xH_2O$, where X can be P, As, and V [13]. The layers are formed by the association of uranyl ions UO_2^{2+} and oxoanions XO_q^{p-}, sharing edges and/or corners. In the phosphorus and arsenic compounds, the uranyl ions UO_2^{2+} are connected by PO_4^{3-} or AsO_4^{3-} tetrahedra, whereas in the vanadium compounds, they are linked by $V_2O_8^{6-}$ units formed by two inverse VO_5 square pyramids sharing an edge. The formed sheets are connected through the interlayer cations and/or water molecules. The same layers $^2_\infty[(UO_2)2V_2O_8]^{2-}$ have been observed for anhydrous compounds with $M^+ = Na^+$, K^+, Cs^+, Ag^+ [3–5,14–16] and for hydrated compounds with $M^{2+} = Ni^{2+}$ [17], Pb^{2+} [18], Ba^{2+} [19], Cu^{2+} [20]. This family derived from the carnotite mineral, presents a relatively high mobility of the alkali metal ions [3,5].

Another type of layer appears with U/V = 1/3 and the structure has been solved for $CsUV_3O_{11}$ [21]. The layers are built from VO_5 square pyramids and $(UO_2)O_6$ hexagonal bipyramids sharing edges and corners, to define an infinite sheets formulated as $^2_\infty[(UV_3O_{11}]^-$ and similar to the layers found in UV_3O_{10} [22]. The mobility of Cs^+ ions sandwiched between two layers seems to be the highest among all the studied uranyl vanadate compounds.

Two new uranyl vanadates families with original layered structures have been recently characterized, the alkali uranyl vanadate family $M_6U_5V_2O_{23}$ (M = Na, K, Rb) [23,24] and the oxychloride compounds $M_7U_8V_2O_{32}Cl$ (M = Rb, Cs) [25]. In these families, the infinite layers $^2_\infty[(UO_2)5(VO_4)2O_5]^{6-}$ and $^2_\infty[(UO_2)8(VO_4)2O_8Cl]^{7-}$ are built from $(UO_2)O_5$ and $(UO_2)O_4Cl$ pentagonal bipyramids, respectively, associated with distorted tetragonal bipyramids $(UO_2)O_4$ and VO_4 vanadium tetrahedra. This tetrahedral coordination for V^{5+} is most prevalent and it was also observed in other mixed uranyl oxyanion compounds, such $U_2V_2O_{11}$ which can be structurally considered as a uranyl divanadate $(UO_2)_2V_2O_7$, where the V_2O_7 units are built from two VO_4 tetrahedra sharing a corner [26,27]. The same structural arrangement was also observed in the uranyl phosphate $Na_2(UO_2)_2P_2O_7$ [28].

However, in the pentahydrated uranyl orthovanadate, $(UO_2)_3(VO_4)_2 \cdot 5H_2O$ [29], the infinite uranyl vanadate layers $^2_\infty[UO_2(VO_4)]^{2-}_2$ are built from $(UO_5)_\infty$ infinite chains of edge-shared uranyl pentagonal bipyramids linked together by VO_4 tetrahedra. An analog structure has been recently described for the tetrahydrated uranyl orthophosphate $(UO_2)_3(PO_4)_2 \cdot 4H_2O$ [30]. The connection between the layers is achieved by disordered $(UO_2)^{2+}$ uranyl ions and water molecules.

The thermal studies of the orthovanadate compound showed that the dehydration to $(UO_2)_3(VO_4)_2$ is reversible, so, it seems that the bidimensional character of the structure is preserved in the anhydrous form. With the aim of obtaining new phases, ion exchange reactions, using $(UO_2)_3(VO_4)_2$ as precursor, may lead to new families. To achieve this objective, attempts at ion exchange reactions have been investigated in different molten alkaline salts. We noted that the use of molten alkaline chlorides allowed the synthesis of orange single crystals of $M_6U_5V_2O_{23}$ phases for M = Na, K [23], and yellow single crystals of $M_7U_8V_2O_{32}Cl$ for M = Rb, Cs [25]. Whereas if the reaction is carried out in rubidium iodide, single crystals of $Rb_6U_5V_2O_{23}$ were prepared [24]. Thus, it seems that the nature of the molten salt, take an important part in the crystallization of new phases. Attempts to prepare single crystals of $Cs_6U_5V_2O_{23}$ using molten cesium nitrate gave a new compound, $Cs_4[(UO_2)_2(V_2O_7)O_2]$. This work is thus devoted to the synthesis and the crystal structure determination of this novel compound. Electrical properties are also reported and compared to those of other cesium uranyl vanadates.

2. Experimental

2.1. Synthesis

For the single-crystal growth, a mixture of uranyl orthovanadate pentahydrated $(UO_2)_3(VO_4)_2 \cdot 5H_2O$ prepared as described in Ref. [29], with a large excess of cesium nitrate (U/Cs = 1/30) is slowly heated in a platinum crucible (1°/min) and maintained at 980°C for 3 days using a tubular furnace. After quenching in air, the molten mixture was washed with water to dissolve the excess of cesium nitrate, giving orange single crystals of $Cs_4[(UO_2)_2(V_2O_7)O_2]$. The powder X-ray diffraction of crushed crystals, using a Guinier-de-Wolff focusing camera with Cu$K\alpha$ radiation, evidenced a pattern diffraction of a new compound.

Pure $Cs_4[(UO_2)_2(V_2O_7)O_2]$ powder was synthesized at 650°C by a solid-state reaction between a stoichiometric mixture of V_2O_5 (Aldrich), U_3O_8 (Prolabo) and Cs_2CO_3 (Aldrich) according to the following reaction:

$$\tfrac{2}{3}U_3O_8 + V_2O_5 + 2Cs2CO_3 + \tfrac{1}{3}O_2 \rightarrow Cs_4[(UO_2)_2(V_2O_7)O_2] + 2CO_2.$$

The homogeneous mixture was slowly heated at 650°C for 7 days in a platinum crucible with several intermediate grindings. The X-ray diffraction pattern of the as-obtained powder is identical to that of crushed

single crystals and to that of calculated pattern from crystal structure results. The unit cell parameters were refined by a least-squares procedure from the indexed powder diffraction pattern, collected with a SIEMENS D5000 diffractometer (Cu$K\alpha$ radiation) equipped with a back-end monochromator and corrected for $K\alpha_2$ contribution. The figure of merit, as defined by Smith and Snyder [31] was $F_{20} = 34.2(0.015; 39)$. The powder X-ray diffraction pattern data are reported in Table 1.

The density measured with an automated Micromeritics Accupy 1330 helium pycnometer using a 1-cm^3 cell, indicates a good agreement between the calculated and measured density, with two formulae by unit cell ($\rho_{mes} = 5.39(2)$ g/cm^3, $\rho_{cal} = 5.38(1)$ g/cm^3 and $Z = 2$).

2.2. Single-crystal X-ray diffraction and structure determination

For the single-crystal X-ray diffraction data collection a well-shaped crystal, of size ($0.036 \times 0.118 \times 0.112$ mm^3), was selected and mounted on an automated BRUKER AXS three circle X-ray diffractometer (Mo$K\alpha$ radiation) equipped with a SMART charge-coupled device detector, with a crystal-to-detector distance of 4.5 cm. The individual frames were collected using a ω-scan technique with an omega rotation of 0.3° and an acquisition time of 40 s per frame. The integral intensities were extracted from the collected frames with the Bruker Saint Plus 6.02 software package [32] using a narrow-frame integration algorithm. A Gaussian-type absorption correction based on precise faces indexing was then applied using XPREP program of the SHELXTL package [33] followed by SADABS [34] for additional corrections. Crystal data, conditions of data collection, and structure refinement parameters are reported in Table 2.

Systematic absences of ($h\,k\,0$, $h + k = 2n + 1$) reflections revealed three possible space groups, $P2_1mn$, $Pm2_1n$ and $Pmmn$. The crystal structure was successfully solved in the centrosymmetric $Pmmn$ space group, by direct methods using SHELXS program [35] that localize the heavy atoms, U and Cs. The positions of vanadium and oxygen atoms were deduced from subsequent refinements and difference Fourier syntheses using the SHELXL option of the SHELXTL software [33]. The atomic scattering factor for neutral atoms were taken from the "International Tables for X-ray Crystallography" [36]. Refinement of atomic positional parameters, anisotropic displacement for U, Cs, V and oxygen atoms, yielded to the final refinement factor ($R = 0.027$) for 636 independent reflections. The atomic positions with equivalent isotropic displacement parameters and anisotropic displacement parameters are reported in Tables 3 and 4, respectively. Table 5 provides the most significant distances and bond valence sums calculated using Brese and O'Keeffe data [37] with

Table 1
Observed and calculated X-ray powder diffraction pattern of $Cs_4[(UO_2)_2(V_2O_7)O_2]$

$h\,k\,l$	d_{obs} (Å)	$2\theta_{obs}$ (deg)	$2\theta_{cal}$ (deg)	I (%)
1 1 0	7.1610	12.35	12.33	54
0 0 1	7.1208	12.42	12.39	19
0 2 0	6.7271	13.15	13.16	8
0 1 1	6.2981	14.05	14.04	4
0 2 1	4.8916	18.12	18.11	9
1 3 0	3.9604	22.43	22.41	8
2 0 1	3.6464	24.39	24.39	35
0 0 2	3.5687	24.93	24.94	36
2 1 1	3.5146	25.32	25.29	24
1 3 1	3.4621	25.71	25.69	14
0 4 0	3.3582	26.52	26.49	31
2 2 1	3.2030	27.83	27.81	100
0 2 2	3.1498	28.31	28.29	66
1 4 0	3.1239	28.55	28.53	6
0 4 1	3.0405	29.35	29.34	12
2 3 1	2.8289	31.60	31.60	14
0 3 2	2.7911	32.04	32.03	6
2 1 2	2.6743	33.48	33.46	7
1 5 0	2.5637	34.97	34.97	2
2 4 1	2.4707	36.33	36.32	9
0 4 2	2.4467	36.7	36.7	9
1 5 1	2.4106	37.27	37.23	3
3 3 0	2.3902	37.60	37.58	3
2 3 2	2.3352	38.52	38.58	2
3 3 1	2.2673	39.72	39.72	5
0 6 0	2.2408	40.21	40.2	7
1 6 0	2.1661	41.66	41.64	4
0 5 2	2.1474	42.04	42.03	5
0 6 1	2.1372	42.25	42.23	6
2 4 2	2.1205	42.60	42.62	21
1 5 2	2.0833	43.40	43.43	9
1 6 1	2.0737	43.61	43.61	17
4 2 0	2.0230	44.76	44.77	5
2 6 0	1.9815	45.75	45.75	13
0 4 3	1.9426	46.72	46.74	4
2 6 1	1.9087	47.60	47.58	11
0 6 2	1.8971	47.91	47.89	8.3
1 7 0	1.8739	48.54	48.55	2
1 6 2	1.8517	49.16	49.75	2
4 0 2	1.8219	50.02	49.99	5
4 4 0	1.7934	50.87	50.86	12
0 5 3	1.7827	51.2	51.23	12
2 4 3	1.7653	51.74	51.73	20
4 2 2	1.7587	51.95	51.93	19
4 4 1	1.7403	52.54	52.56	7
1 1 4	1.7321	52.81	52.84	6
0 2 4	1.7236	53.09	53.07	10
0 8 0	1.6812	54.54	54.55	4
0 8 1	1.6364	56.16	56.17	5
1 6 3	1.6020	57.48	57.48	6
3 6 2	1.5752	58.55	59.52	4
4 6 0	1.5403	60.01	60.00	4
4 6 1	1.5065	61.50	61.53	3
2 4 4	1.4772	62.86	62.86	5
2 8 2	1.4313	65.12	65.11	7
6 0 0	1.4139	66.02	66.02	4
0 6 4	1.3958	66.99	66.99	4
2 9 1	1.3796	67.88	67.71	3
4 0 4	1.3653	68.69	68.70	4
0 3 5	1.3589	69.06	69.01	7
2 0 5	1.3522	69.45	69.43	4
4 2 4	1.3379	70.30	70.31	7

a=8.482(1) Å, b=13.448(1) Å, c=7.125(1) Å, $F_{20} = 34.2(0.015; 39)$.

Table 2
Crystal data, intensity collection and structure refinement parameters for $Cs_4[(UO_2)_2(V_2O_7)O_2]$

Crystal data				
Crystal symmetry	Orthorhombic			
Space group	*Pmmn*			
Unit cell parameters refined from single crystal data	$a = 8.4828(15)$ Å			
	$b = 13.426(2)$ Å			
	$c = 7.1366(13)$ Å			
	$V = 812.8(3)$ Å^3			
Z	2			
Calculated density	$\rho_{cal} = 5.38(1)$ g/cm^3			
Measured density	$\rho_{mes} = 5.39(2)$ g/cm^3			
Data collection				
Temperature (K)	293(2)			
Equipment	Bruker SMART CCD			
Radiation Mo$K\alpha$	0.71073 Å			
Scan mode	ω			
Recording angular range (deg)	2.84–23.23			
Recording reciprocal space	$-9 \leqslant h \leqslant 9$			
	$-14 \leqslant k \leqslant 14$			
	$-7 \leqslant l \leqslant 7$			
No. of measured reflections	3014			
No. of independent reflections	636			
μ (cm^{-1}) (for $\lambda_{K\alpha} = 0.71073$ Å)	298.57			
Limiting faces and distances (mm) from an arbitrary origin	1 0 0	0.018	−1 0 0	0.018
	0 1 0	0.059	0 −1 0	0.059
R merging factor	0 0 1	0.056	0 0 −1	0.056
	0.051			
Refinement				
Refined parameters/restraints	62/0			
Goodness of fit on F^2	1.085			
$R_1[I > 2\sigma(I)]$	0.027			
wR_2 $[I > 2\sigma(I)]$	0.066			
R_1 for all data	0.029			
wR_2 for all data	0.069			
Largest diff. Peak/hole (e/Å^3)	2.48/−1.45			

$R_1 = \sum(|F_o| - |F_c|)/\sum|F_o|$.
w$R_2 = [\sum w(F_o^2 - F_c^2)^2/\sum w(F_o^2)^2]^{1/2}$.
$w = 1/[\sigma^2(F_o^2) + (aP)^2 + bP]$ where a and b are refinable parameters and $P = (F_o^2 + 2F_c^2)/3$.

Table 3
Atomic coordinates and equivalent displacement parameters (Å^2) of $Cs_4[(UO_2)_2(V_2O_7)O_2]$

Atom	Site	x	y	z	U_{eq}
U	4*c*	0	1/2	0	0.0099(3)
V	4*f*	−0.0455(4)	3/4	0.2975(5)	0.0133(8)
Cs1	4*e*	1/4	0.5449(1)	−0.5130(2)	0.0254(4)
Cs2	2*b*	1/4	3/4	−0.1271(3)	0.0215(6)
Cs3	2*a*	1/4	1/4	0.2058(3)	0.0242(6)
O1	4*f*	1/4	0.5135(9)	−0.021(2)	0.026(4)
O2	8*g*	−0.019(1)	0.5708(8)	−0.219(1)	0.020(3)
O3	8*g*	−0.001(1)	0.6474(7)	0.170(2)	0.031(3)
O4	4*f*	0.058(2)	3/4	0.486(2)	0.020(3)
O5	2*a*	−1/4	3/4	0.359(3)	0.033(6)

Note: The U_{eq} values are defined by $U_{eq} = 1/3(\sum_i \sum_j U_{ij} a_i^* a_j^* a_i a_j)$.

$b = 0.37$ Å except for U–O bonds where the coordination-independent parameters ($R_{ij} = 2.051$ Å, $b = 0.519$ Å) were taken from Burns et al. [38].

2.3. Electrical conductivity measurements and thermal analyses

Electrical conductivity measurements were carried out on cylindrical pellets obtained using a conventional cold press and sintered at 700°C for 2 days, followed by very slow cooling, 2°/h, until room temperature. Gold electrodes were vacuum deposited on both flat surfaces of the pellets. Conductivity measurements were performed by AC impedance spectroscopy over the range 1–10^6 Hz with a Solartron 1170 frequency-response analyzer. Measurements were made at 20°C intervals over the range 250–900°C on both heating and cooling. Each set of values were recorded at a given temperature after a 1 h stabilization time.

Differential thermal analysis (DTA) was conducted in air on SETARAM DTA. 92–1600 apparatus thermal analyzer, between 20°C and 1100°C with heating or cooling rate 2°/mn, using platinum crucible.

Table 4
Anisotropic displacement parameters (Å^2) of $Cs_4[(UO_2)_2(V_2O_7)O_2]$

Atom	U_{11}	U_{22}	U_{33}	U_{12}	U_{13}	U_{23}
U1	0.0067(4)	0.0081(5)	0.0151(5)	0.0008(3)	−0.0002(4)	−0.0008(4)
Cs1	0.0197(7)	0.0324(10)	0.0243(9)	0	0	−0.0062(7)
Cs2	0.0212(9)	0.0166(9)	0.0269(9)	0	0	0
Cs3	0.0224(9)	0.0167(9)	0.0336(9)	0	0	0
V1	0.017(2)	0.008(2)	0.015(2)	0	−0.0003(1)	0.00000
O1	0.013(8)	0.033(11)	0.033(10)	0	0	0.000(8)
O2	0.018(5)	0.018(7)	0.025(6)	−0.003(4)	0.005(5)	0.003(5)
O3	0.038(6)	0.010(6)	0.045(8)	−0.001(5)	0.006(6)	−0.019(6)
O4	0.026(8)	0.017(9)	0.017(9)	0	−0.001(8)	0
O5	0.017(12)	0.045(16)	0.038(16)	0	0	0

Note: The anisotropic displacement factor exponent takes the form $-2\pi^2[h^2a^{*2}U_{11} + k^2b^{*2}U_{22} + l^2c^{*2}U_{33} + \cdots + 2\,h\,k\,a^*b^*U_{12}]$.

Table 5
Selected bond distances (Å) and bond valences for $Cs_4[(UO_2)_2(V_2O_7)O_2]$

Atom	Distance	s_{ij}	Atom	Distance	s_{ij}
Uranium environment			*Vanadium environment*		
U–O2(2 ×)	1.838(11)	1.507	V–O4	1.605(15)	1.708
U–O1(2 ×)	2.134(2)	0.852	V–O3(2 ×)	1.694(10)	1.343
U–O3(2 ×)	2.321(10)	0.594	V–O5	1.793(6)	1.027
$\sum s_{ij}$		*5.906*	$\sum s_{ij}$		5.420
Uranyl angle (deg)					
O2–U1–O2^i = 180.0(4)					
Cesium environments					
Cs1–O2(2 ×)	3.118(10)	0.150	Cs2–O4(2 ×)	3.207(14)	0.118
Cs1–O2(2 ×)	3.148(10)	0.139	Cs2–O1(2 ×)	3.264(15)	0.101
Cs1–O4(2 ×)	3.203(8)	0.120	Cs2–O3(4 ×)	3.304(11)	0.091
Cs1–O3(2 ×)	3.403(11)	0.071	Cs2–O2(4 ×)	3.381(10)	0.074
Cs1–O1	3.536(14)	0.048	$\sum s_{ij}$		*1.098*
Cs1–O1	3.651(14)	0.048			
$\sum s_{ij}$		*1.044*			
Cs3–O5	3.092(22)	0.162			
Cs3–O2(4 ×)	3.104(10)	0.156			
Cs3–O4	3.413(14)	0.068			
Cs3–O3(4 ×)	3.681(11)	0.033			
$\sum s_{ij}$		*1.054*			

High-temperature X-ray diffraction (HTRXD) was carried out using a Guinier–Lenné focusing camera with Cu$K\alpha$ radiation in the range from room temperature to 800°C.

3. Crystal structure description and discussion

The structure of $Cs_4[(UO_2)_2(V_2O_7)O_2]$ consists of two-dimensional $^2_\infty[(UO_2)2(V_2O_7)O_2]^{4-}$ layers separated by Cs^+ cations. The layers are formed from UO_6 tetragonal bipyramids and VO_4 tetrahedra, as shown in Fig 1. For a better understanding of the structural chemistry, the layers can be described from two fragments. First, the UO_6 tetragonal bipyramids are associated by sharing opposed corners O(1) to give infinite chains $^1_\infty[UO_5]^{4-}$ parallel to *a*-axis. In addition, divanadate groups V_2O_7 are obtained from two tetrahedra sharing a corner O(5). Finally, two parallel $^1_\infty[UO_5]^{4-}$ chains are linked together by the divanadate groups which share four O(3) oxygen atoms, two with each chain, this linkage repeats along the *b*-axis to form the infinite layers $^2_\infty[(UO_2)_2(V_2O_7)O_2]^{4-}$ that are parallel to the (001) plane. Within a layer, the V_2O_7 entities are parallel to the $^1_\infty[UO_5]^{4-}$ chains. All the V_2O_7 vanadate groups that connect one side of an $^1_\infty[UO_5]^{4-}$ uranyl chain are *pointed down*, whereas all the tetrahedra along the other side of the same uranyl chain *pointed up*, leading to a structure with a piling of corrugated layers (Fig. 2). The interlayer space is occupied by the cesium atoms.

Linkage of $^1_\infty[UO_5]^{4-}$ chains by divanadate groups to form layers is quite unusual. Such chains formed from

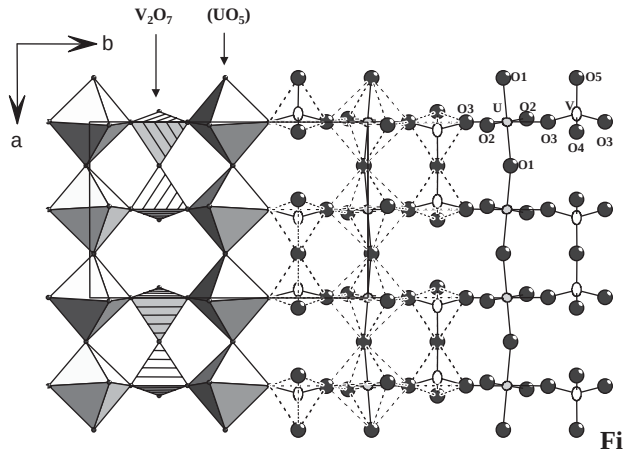

Fig. 1. Part of the two-dimensional $^{2}_{\infty}[(UO_2)_2(V_2O_7)O_2]^{4-}$ layers in $Cs_4[(UO_2)_2(V_2O_7)O_2]$ built from $^{1}_{\infty}[UO_5]^{4-}$ chains of corner-sharing UO_6 tetragonal bipyramids connected through V_2O_7 divanadate groups.

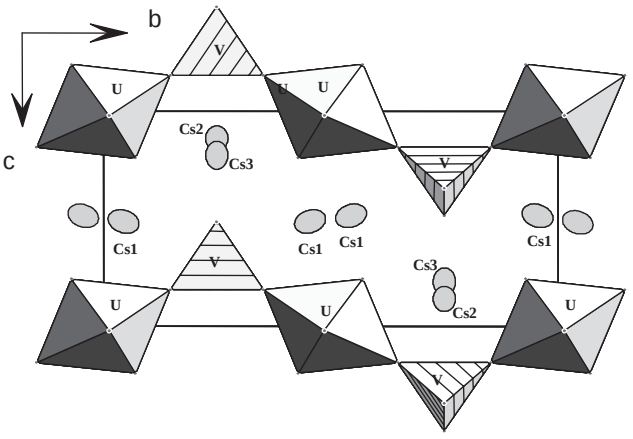

Fig. 2. Projection of the crystal structure of $Cs_4[(UO_2)_2(V_2O_7)O_2]$ on (100) plane showing the corrugated $^{2}_{\infty}[(UO_2)2(V_2O_7)O_2]^{4-}$ layers and interlayer Cs atoms.

corner-shared UO_6 tetragonal bipyramids are present in alkaline and alkaline earth uranates of the type $M^{n+}_{4/n}[(UO_2)O_3]$ with $M^{+}=Li^{+}$ [39], Na^{+} [40], and $M^{2+}=Sr^{2+}$, Ca^{2+} [41]. In these compounds, the cohesion between the chains is only insured by the alkaline or alkaline earth cations. Such chains also occur in the structure of β and γ uranyl hydroxides $UO_2(OH)_2$ [42,43] and in several monouranates of general formula $M^{n+}_{2/n}[(UO_2)O_2]$ with $M=$Li [44], Na [45], Sr [41], Ba [46], Pb [47]. In these compounds, the chains are directly connected together to form $^{2}_{\infty}[UO_4]^{2-}$ layers. In $U_2V_2O_{11}$, $^{1}_{\infty}[UO_5]^{4-}$ chains are connected by V_2O_7 groups, but in this compound the chains are built from UO_7 pentagonal bipyramids sharing opposite edges [26,27].

The unique independent uranium atom U is bonded to two symmetrical oxygen atoms O(2), at short distances 1.839(11) Å, forming a perfectly linear uranyl ion UO_2^{2+} [U–O–U = 180.0(4)°] which is surrounded in equatorial plane by a square environment of opposed oxygen atoms, two O(1) and two O(3), situated at 2.134(2) and 2.321(10) Å, respectively. The uranyl U=O bond length is slightly higher than the average value of 1.79 Å calculated by Burns et al. [38]; however, for U^{6+} in distorted octahedral environment, the uranium–oxygen bond length varying in considerably, e.g., short distances (1.75(1) and 1.77(1) Å) are observed in $K_2[(UO_2)_2(VO)_2(IO_6)_2O]\cdot H_2O$ [48], while long distances are obtained in alkaline uranates (e.g., 1.996 Å in Li_4UO_5 [39]). The presence of uranyl bonds is not evident in some distorted octahedra as in Ca_3UO_6 or Sr_3UO_6 with U–O distances ranging from 2.023 to 2.181 Å) [41]. In $Cs_4[(UO_2)_2(V_2O_7)O_2]$, the equatorial oxygen form a diamond shape, the shortest distances corresponding to the oxygen that is not shared with vanadium.

The unique independent vanadium atom is surrounded by a very distorted tetrahedral environment of oxygen atoms O(5), O(4) and two O(3) at 1.793, 1.605 and 1.694 Å, respectively. The longest distance corresponds to the oxygen shared between two VO_4 tetrahedra to form the divanadate unit, the intermediate one is for oxygen shared with UO_6 bipyramids, the shortest is for the oxygen that does not participate to the layer building. The V–O(5)–V angle is 150.7(2)°.

Cs(1) and Cs(3) atoms are surrounded by 10 oxygen atoms in a range 3.118–3.651 Å and 3.092–3.6681 Å, respectively; whereas Cs(2) atom is coordinated by 12 oxygen atoms in the range 3.208–3.379 Å.

On the basis of the U–O, V–O and Cs–O bond lengths, bond valence sums were calculated to be 5.91, 5.42, 1.04, 1.10, 1.05 for U, V, Cs(1), Cs(2) and Cs(3), respectively. These values are in agreement with the expected values except for V which seems over-bonded due to the short V–O(4) bond. Bond valence sums for the O atoms range from 1.89 to 2.13.

To evidence the interlayer mobility of alkaline ions, electrical conductivity measurements were carried out. Thus, Fig. 3 indicates the temperature dependence of the electrical conductivity of $Cs_4[(UO_2)_2(V_2O_7)O_2]$ compound, compared with three known cesium uranyl vanadates: the carnotite $Cs_2[(UO_2)_2V_2O_8]$, the cesium uranyl trimetavanadate $Cs[UO_2(VO_3)_3]$, and the cesium uranyl oxychlorovanadate $Cs_7[(UO_2)_8(VO_4)_2O_8Cl]$. For $Cs_4[(UO_2)_2(V_2O_7)O_2]$, the electrical conductivity evolution agrees with the Arrhenius law in both parts of the curve which presents a jump between 635°C and 680°C. At low temperatures, the electrical conductivity is lower than for the three other compounds. Whereas, for the temperatures higher than 680°C, the conductivity becomes more important and is of the same order as that of the carnotite. The activation energy is about 0.73 eV in both temperature domains.

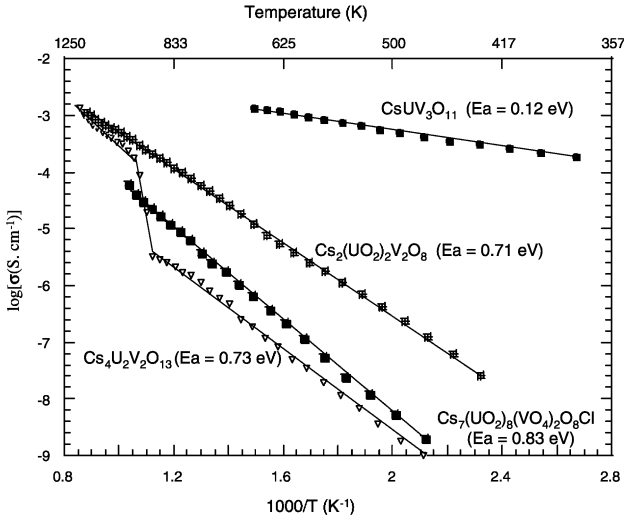

Fig. 3. Comparison between $Cs_4[(UO_2)_2(V_2O_7)O_2]$ and other Cs-containing uranyl vanadates conductivity vs. temperature.

To study the origin of this abrupt conductivity variation, two other thermal techniques were used: DTA and HTRXD. In the two experiments, no anomaly was observed, thus this phenomenon is not due to a structural transition. DTA measurement showed the $Cs_4[(UO_2)_2(V_2O_7)O_2]$ congruently melts at 1020°C and powder X-ray diffraction analyses of residue after DTA measurement confirm the existence of only $Cs_4[(UO_2)_2(V_2O_7)O_2]$.

Attempts of synthesis of isotypic compounds with other alkaline elements by solid-state reactions have been investigated from a mixture of M_2CO_3 (M = Na, K, Rb), U_3O_8 and V_2O_5 in molar accounts 2/0.66/1, corresponding to $M_4[(UO_2)_2(V_2O_7)O_2]$. For each compound, the homogeneous mixture was slowly heated (1°/min), in a platinum crucible, and maintained with intermediate grindings 3 days at different temperatures between 550°C and the melting temperature, because before 550°C no reaction was observed. For each sample, the melting point was determined by DTA. In all cases, X-ray diffraction patterns indicate since 650°C, a mixture containing principally $M_6U_5V_2O_{23}$ with M = Na, K, Rb.

Alkaline exchange of the cesium was also tested in different saturated aqueous solutions of alkaline nitrates MNO_3 (M = Na, K, Rb) with a molar ratio M/Cs = 10/1. The solution is heated at 60°C during 1 week under stirring. The color of the powder, initially orange, becomes yellow, indicating a reaction. For M = Na and K, the powder obtained after decantation, filtration and drying, analyzed by X-ray diffraction, is $Cs_2[(UO_2)_2V_2O_8]$. The analysis by energy dispersion spectroscopy (EDS) proves the absence of Na and K in the two phases. The reaction can be resumed as a simple decomposition of the initial phase according to

$$Cs_4[(UO_2)_2(V_2O_7)O_2] + H_2O \rightarrow Cs_2[(UO_2)_2V_2O_8] + 2CsOH.$$

This interpretation is confirmed by attempts in water alone where the Cs analog of carnotite is obtained. This explains why most of the uranyl vanadate minerals belong to the carnotite group. In Rb case, the process is more complicated because the decomposition in cesium carnotite is accompanied by a partial substitution of Cs by Rb indicated by EDS analysis. Single crystals have been synthesized by melting at 800°C of the powder formed after the partial substitution, followed of a slow cooling. The crystal structure refinement confirmed a typical carnotite structure with the formula $Cs_{0.66}Rb_{1.34}(UO_2)_2V_2O_8$.

Thus, until now, $Cs_4[(UO_2)_2(V_2O_7)O_2]$ remains the alone representative of this new layered alkali uranyl vanadates whose layers result from the association of UO_6 octahedra and V_2O_7 divanadate units.

4. Conclusion

The reaction of uranyl orthovanadate $(UO_2)_3(VO_4)_2{\cdot}5H_2O$ in a large excess of molten cesium nitrate does not lead to the expected $Cs_6(UO_2)_5(VO_4)_2O_5$ but to single crystals of a new layered compound, $Cs_4[(UO_2)_2(V_2O_7)O_2]$. It can be directly synthesized by heating the mixture U_3O_8–V_2O_5–Cs_2CO_3 in molar accounts $\frac{2}{3}$–1–2. The layers are particularly original and are constructed from UO_6 distorted octahedra and V_2O_7 divanadate units. $Cs_4[(UO_2)_2(V_2O_7)O_2]$ is until now the lone representative of this layer's type. Attempts of synthesis of Na, K or Rb analogs, either by solid-state reaction or by exchange reaction in aqueous solution, failed; the $M_6U_5V_2O_{23}$ (M = Na, K, Rb) phases are principally obtained by solid-state reaction and cesium analog of the mineral carnotite by "exchange" in nitrate aqueous solution.

References

[1] P.C. Burns, M.L. Miller, R.C. Ewing, Canad. Mineral. 34 (1996) 845.
[2] P.C. Burns, R. Finch (Eds.), Rev. Miner. 38 (1999) 23.
[3] F. Abraham, C. Dion, M. Saadi, J. Mater. Chem. 3 (5) (1993) 459.
[4] F. Abraham, C. Dion, N. Tancret, M. Saadi, Adv. Mater. Res. 1–2 (1994) 511.
[5] M. Saadi, Thesis, Lille, 2001.
[6] Y.F. Yao, J.T. Kummer, J. Inorg. Nucl. Chem. 29 (1967) 2453.
[7] B. Morosin, Phys. Lett. 65A (1978) 53.
[8] A.T. Howe, M.G. Shilton, J. Solid State Chem. 28 (1979) 345.
[9] P.E. Childs, A.T. Howe, M.G. Shilton, J. Solid State Chem. 34 (1980) 341.

[10] C.M. Johnson, M.G. Shilton, A.T. Howe, J. Solid State Chem. 37 (1981) 37.
[11] M. Pham_Thi, Ph. Colomban, Solid State Ionics 17 (1985) 295.
[12] J. Benavente, J.R. Ramos-Barrado, M. Martinez, S. Bruque, J. Appl. Electrochem. 25 (1995) 68.
[13] F. Weigel, G. Hoffmann, J. Less-Common Met. 44 (1976) 99.
[14] P.B. Barton, J. Am. Miner. 43 (1958) 799.
[15] D.E. Appleman, H.T. Evans, J. Am. Miner. 50 (1965) 825.
[16] P.G. Dickens, G.P. Stuttard, R.G.J. Ball, A.V. Powell, S. Hull, S. Patat, J. Mater. Chem. 2 (2) (1992) 161.
[17] J. Borène, F. Cesbron, Bull. Soc. Fr. Miner. Crystallogr. 93 (1970) 426.
[18] J. Borène, F. Cesbron, Bull. Soc. Fr. Miner. Cristallogr. 99 (1971) 8.
[19] D.P. Shashkim, Dokl. Akad. Nauk. SSSR 220 (1974) 1410.
[20] P. Piret, P. Declercq, D. Wauters-Stoop, Bull. Miner. 103 (1980) 176.
[21] I. Duribreux, C. Dion, M. Saadi, F. Abraham, J. Solid State Chem. 146 (1999) 258.
[22] A.M. Chippinade, S.N. Crennell, P.G. Dickens, J. Mater. Chem. 3 (1993) 33.
[23] C. Dion, S. Obbade, E. Raekelboom, M. Saadi, F. Abraham, J. Solid State Chem. 155 (2000) 342.
[24] S. Obbade, C. Dion, L. Duvieubourg, M. Saadi, F. Abraham, J. Solid State Chem. 173 (2003) 1.
[25] I. Duribreux, M. Saadi, S. Obbade, C. Dion, F. Abraham, J. Solid State Chem. 172 (2003) 351.
[26] A.M. Chippinade, P.G. Dickens, G.J. Flynn, G.P. Stuttard, J. Mater. Chem. 5 (1) (1995) 141.
[27] N. Tancret, S. Obbade, F. Abraham, Eur. J. Solid State Inorg. Chem. 32 (1995) 195.
[28] S.A. Linde, Y.E. Gorbunova, A.V. Lavrov, A.B. Pobedina, Zh. Neorg. Khim. 29 (1984) 1533.
[29] M. Saadi, C. Dion, F. Abraham, J. Solid State Chem. 150 (2000) 72.
[30] A.J. Locock, P.C. Burns, J. Solid State Chem. 163 (2002) 275.
[31] G. Smith, R.J. Snyder, J. Appl. Crystallogr. 1212 (1979) 60.
[32] SAINT, Program for Reduction of Data Collected on Bruker AXS CCD Area Detector System, Bruker Analytical X-ray Systems, Madison, WI, 1998.
[33] GM Sheldrick, SHELXTL NT, Program Suite for solution and Refinement of Crystal Structure, version 5.1, Bruker Analytical X-ray Systems, Madison, WI, 1998.
[34] SABABS. Program for Absorption Correction Using SMART CCD Based on the Method of Blessing: Blessing, R.H. Acta Crystallogr. A 51 (1995) 33.
[35] G.M. Sheldrick, SHELXS-98, Program for Crystal Structure Determination, University of Göttingen, Germany, 1986.
[36] J.A. Ibers, W.C. Hamilton, International Tables for X-ray Crystallography, Vol. IV, Kynoch Press, Birmingham, UK, 1974.
[37] N.E. Brese, M. O'Keeffe, Acta Crystallogr. B 47 (1991) 192.
[38] P.C. Burns, R.C. Ewing, F.C. Hawthorne, Can. Miner. 35 (1997) 1551.
[39] K.V. Reshetov, L.M. Kovba, J. Struct. Chem. 7 (1966) 589.
[40] R. Wolf, R. Hoppe, Rev. Chim. Minér. 23 (1986) 828.
[41] B.O. Loopstra, H.M. Rietveld, Acta Crystallogr. B 25 (1969) 787.
[42] J.C. Taylor, M.J. Bannister, Acta Crystallogr. B 28 (1972) 2995.
[43] S. Siegel, H.R. Hoekstra, Acta Crystallogr. B 28 (1972) 3469.
[44] E. Gebert, H.R. Hoekstra, A.H. Reis, S.W. Peterson, J. Inorg. Nucl. Chem. 40 (1978) 65.
[45] L.M. Kovba, Radiokhimiya 13 (1971) 309.
[46] A.H. Reis, H.R. Hoekstra, E. Gebert, S.W. Peterson, J. Inorg. Nucl. Chem. 38 (1976) 1481.
[47] T.L. Cremers, P.G. Eller, E.M. Larson, A. Rosenzweig, Acta Crystallogr. C 42 (1986) 1684.
[48] R.E. Sykora, T.E. Albrecht-Schmitt, Inorg. Chem. 42 (2003) 2179.